

Negative Temperature States in the Discrete Nonlinear Schrödinger Equation

S. Iubini,^{1,2} R. Franzosi,² R. Livi,¹ G.-L. Oppo,³ and A. Politi^{4,2}

¹*Dipartimento di Fisica e Astronomia – CSDC, Università di Firenze and INFN Sezione di Firenze, via Sansone 1, I-50019 Sesto Fiorentino, Italy*

²*CNR - Istituto dei Sistemi Complessi, via Madonna del Piano 10, I-50019 Sesto Fiorentino, Italy*

³*ICS, SUPA and Department of Physics, University of Strathclyde, 107 Rottenrow, Glasgow G4 0NG, U.K.*

⁴*ICSMB, SUPA and Department of Physics, University of Aberdeen AB24 3UE, U.K.*

We explore the statistical behavior of the discrete nonlinear Schrödinger equation. We find a parameter region where the system evolves towards a state characterized by a finite density of breathers and a negative temperature. Such a state is metastable but the convergence to equilibrium occurs on astronomical time scales and becomes increasingly slower as a result of a coarsening processes. Stationary negative-temperature states can be experimentally generated via boundary dissipation or from free expansions of wave packets initially at positive temperature equilibrium.

PACS numbers: 63.70.+h, 05.45.-a, 03.75.Lm, 42.65.Tg

The discrete nonlinear Schrödinger (DNLS) equation has been widely investigated as a semiclassical model for Bose-Einstein condensates (BEC) in optical lattices and for light propagation in arrays of optical waveguides [1]. It exhibits peculiar solutions in the form of lattice solitons, also known as breathers, or intrinsically localized nonlinear excitations [2]. In the first statistical-mechanics study of the DNLS equation, Rasmussen *et al.* [3] identified a region R_n in the parameter space that was conjectured to be characterized by negative temperature (NT) states. NT states have attracted the curiosity of researchers since pioneering works in systems of quantum nuclear spins [4]. In a series of recent papers, Rumpf argued that there are no NT equilibrium states in R_n . In fact, he showed that the maximum entropy (i.e. equilibrium) state is characterized by an infinite-temperature background superposed to a single breather that collects the “excess” energy [5]. Convergence to such equilibrium states, however, has never been observed, since the transient may last for astronomical times [10]. Therefore it is legitimate to ask what happens over physically accessible time scales. The occurrence of long transients is not rare in statistical mechanics: it may be due to coarsening, nucleation, presence of free-energy barriers, or the stability of some modes. Within the physical setups that are closest to the DNLS, a nonexponential relaxation was first found in chains of nonlinear oscillators and shown to originate from the presence of long-lived localized solutions [6]. Slow relaxations have been also found in Heisenberg spin chains and traced back to the existence of two conservation laws [7]. This latter example is particularly instructive, since it is the context where theoretical arguments, later applied to the DNLS, have been developed. The approach is well suited for the identification of the equilibrium state by maximizing the entropy given the constraints imposed by the conservation laws. It is however of little help to investigate the convergence properties to equilibrium. In this respect, the implementation of a microcanonical Monte Carlo (MMC) method turns

out to be quite useful, in that it allows uncovering (in the so-called weak-coupling limit) a first source of “slowness” in an underlying coarsening phenomenon that follows from the subdiffusive behavior of the breather amplitude. As a result, we find that the density of breathers vanishes in time as $t^{-\alpha}$ with an exponent $\alpha \approx 0.37$ that is reminiscent of the exponent $1/3$ of the Cahn-Hilliard model [8]. Note, however, that dynamical mechanisms which strongly inhibit the diffusion of the breather amplitude are even more effective. With the help of an explicit expression for the microcanonical temperature [9], we are able to show that a broad class of initial conditions (IC) of the DNLS equation converges towards a well defined thermodynamic state characterized by a negative temperature and a finite density of breathers. There is no reason to dismiss the theoretical arguments of [5], although it appears that the dynamical freezing of the high-amplitude breathers slows down the evolution so much to make the convergence to equilibrium unobservable. Altogether this phenomenon is reminiscent of aging in glasses, but a more detailed analysis is required to frame the analogy on more firm grounds. Finally, we briefly comment on a simple strategy to generate experimentally metastable NT states in BEC in optical lattices and in arrays of optical waveguides. Our scheme is far simpler than the thermalization methods recently proposed for BEC trapped in lattices which require non-trivial Mott states followed by sweeps across Feshbach resonances to invert the sign of the atomic interaction [12].

Model and state of the art. With reference to the standard canonical coordinates, the Hamiltonian of a DNLS chain writes

$$H(p, q) = \sum_j (p_j^2 + q_j^2)^2 + 2 \sum_j (p_j p_{j+1} + q_j q_{j+1}), \quad (1)$$

where the index j numbers the sites from 1 to N and periodic boundary conditions are assumed. The sign of the first term in the r.h.s. is assumed to be positive, since

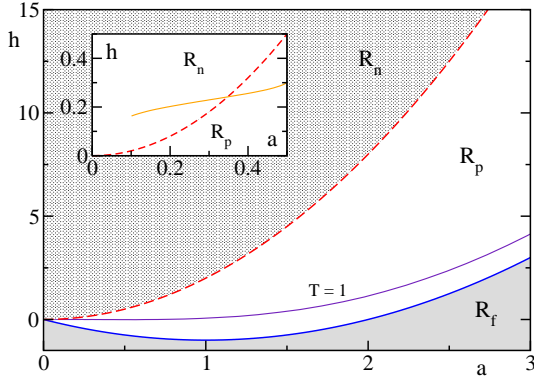


FIG. 1: (Color online) Phase diagram (a, h) [3]. We show the isothermal lines $T = 0$ (solid blue), $T = 1$ (solid purple) and $T = \infty$ (dashed red). In the inset: average trajectory (over an ensemble of 500 realizations) of a chain with $N = 200$ in the presence of boundary dissipation.

we refer to the case of a repulsive-atom BEC, while the sign of the hopping term is irrelevant, due to the symmetry associated with the canonical (gauge) transformation $\phi_j \rightarrow \phi_j + \pi$ (where $p_j + iq_j \equiv u_j e^{i\phi_j}$ represents the wave function at site j). The model possesses two conserved quantities: the energy H and the number of particles (or, wave action) $A = \sum_j u_j^2$. The thermodynamic properties of this model are summarized in a phase-diagram of energy (h) versus particle (a) density per site [3]. In Fig. 1, one can identify three regions: (i) a forbidden region R_f , that lies below the ground state; (ii) an intermediate positive temperature R_p region; (iii) the above mentioned region R_n , that is investigated in this Letter. The presence of low relaxation phenomena in R_n was first noticed in [3] by monitoring the probability density of the local amplitudes $A_j \equiv u_j^2$. The reason was traced back to the presence of breathers (that arise as a result of a modulational instability [7, 13]) and attributed to the weakness of their coupling to the background.

Microcanonical Monte Carlo simulations. We start our analysis of DNLS dynamics from the weak-coupling limit (i.e. large particle densities). In this regime, the region R_n corresponds to $h/a^2 > 2$ [5] (with our normalizations). The motivation for a MMC study is a direct investigation of entropic effects during the time evolution. In order to mimic the deterministic evolution, we have introduced a local updating rule which applies to a randomly selected triplet of consecutive sites. Since it is necessary to leave the number of particles $A_j^s = A_{j-1} + A_j + A_{j+1}$ and the energy $H_j^s = A_{j-1}^2 + A_j^2 + A_{j+1}^2$ unchanged, the new configuration must lie along the intersection between a plane and the surface of a sphere, while restricted to the positive octant ($A_j \geq 0$). Depending on the relative amplitude of H_j^s and A_j^s , this line may be either a full circle or made of three separate arcs. In the former case, we select a point on the circle (assuming uniform probability); in the latter one, we select a point within

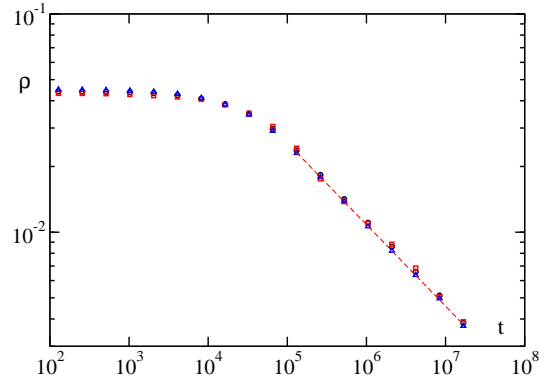


FIG. 2: (Color online). Average breather density ρ versus time t in a DNLS chain as from MMC simulations in the weak-coupling limit. Circles, squares and triangles refer to $N = 400, 1600$, and 6400 , respectively. The straight line with slope 0.37 is the result of a power-law fit.

the same arc as of the IC. It is easy to verify that detailed balance is satisfied. After having observed that the above algorithm yields a fast convergence towards the expected equilibrium state in the $T > 0$ region, we have performed some simulations in R_n . The IC is fixed by assigning a random amplitude A_j (with a flat distribution between 0 and 1) to all sites and adding $40/3$ units to 5% of sites randomly chosen over the chain. This choice implies that $h/a^2 \approx 7 > 2$, i.e. the IC lies inside R_n . In Fig. 2 we plot the MMC evolution of the fraction ρ of sites, where the amplitude A_j is larger than the threshold $\eta = 10$ [14] for three different system sizes [15]. The three curves nicely overlap and show for large time t a clear power-law decay $\rho \sim t^{-\alpha}$, with an exponent $\alpha \approx 0.37$. Time t is given by the number of MMC steps divided by N . This means that the system converges, although slowly, to the equilibrium state characterized by a single breather (i.e. $\rho = 0$ in the thermodynamic limit). In order to gain further insight, we have looked at the MMC evolution in two different ways. In Fig. 3a, we plot the position of the breathers of amplitude larger than η . The breathers are basically static and either terminate abruptly, or eventually exhibit a weak mutual attraction. The representation in panel Fig. 3b is more illuminating. There, we plot the sum of the “excess” energies $H_j^* = \sum_{l=1}^j (A_l^2 - \eta^2) \theta(A_l^2 - \eta^2)$ (θ is the Heaviside function) in correspondence of each breather. The abscissa of the rightmost breather is the total excess energy contained in the breathers. After an initial transient during which the excess energy is constant, the breathers perform a sort of Brownian motion in energy space until they collide and merge. This (sub)diffusive motion reveals a slow convergence that is due to a likewise coarsening phenomenon. It is intriguing to see that the value of α (0.37) is relatively close to the critical exponent of the Cahn-Hilliard equation ($1/3$). We leave the task of identifying the correct universality class to future

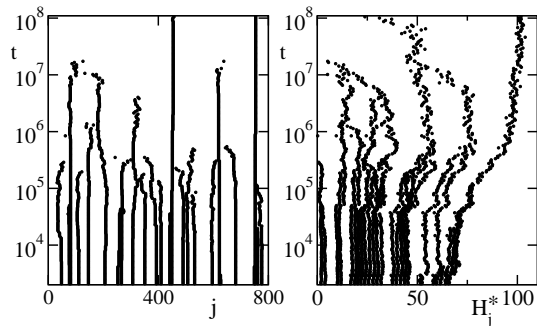


FIG. 3: (a) Space time representation of MMC dynamics of breathers in the NT region. (b) Same as in panel a, with the label j replaced by H_j^* , see text.

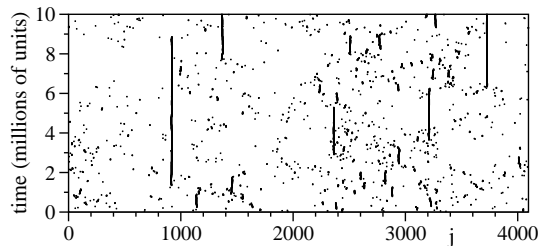


FIG. 4: Evolution of the local amplitude in an NT states (dots correspond to points where $A_j > 10$) for $a = 1$ and $h = 2.4$.

investigations.

DNLS Dynamics. The MMC study has shown that in the weak-coupling limit, the convergence is characterized by a coarsening process: the fewer the breathers, the weaker their interaction and the slower the convergence process. The uncoupled limit is, however, rather peculiar, as it lacks the hopping mechanism. In the natural case of a finite coupling, we have turned our attention to simulations of the deterministic DNLS since effective implementations of MMC rules are not feasible. Fig. 4 presents the space-time evolution for a chain of 4096 sites for $a = 1$ and $h = 2.4$. To emphasize the breather dynamics, we plot only the lattice points, where the instantaneous mass A_j is larger than $\eta = 10$. Thanks to a symplectic 4th-order algorithm of Yoshida type [16], we have simulated the dynamics over time scales much longer than in the previous numerical studies. In Fig. 4 one can see that, like in the MMC simulations, the breathers do not basically move; at variance with the uncoupled case, however, we observe spontaneous birth and death of breathers as in a standard stationary process. This is due to the presence of a finite interaction (hopping) energy: the background can store excess energy in the phase differences of neighbouring sites and this implies that breathers can spontaneously nucleate. In order to better investigate the convergence properties of the dynamics, we have built four different sets of ICs, all with the same energy and number of particles but substan-

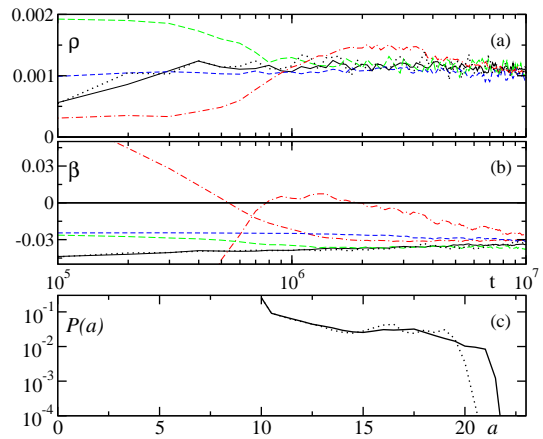


FIG. 5: (Color online) Evolution for $a = 1$, $h = 2.4$ of (a) the breather density ρ and (b) the inverse temperature $\beta = 1/T$ starting from different ICs for a chain with $N = 4096$: solid, long-dashed and dashed lines refer to a suitable homogeneous background plus 0, 4 (amplitude 20) and 8 (amplitude 16) breathers, respectively, while the dot-dashed curves refer to half a chain empty. Both ρ and β are averaged over a moving window of 10^5 time units. Notice that in panel (b) the two dot-dashed lines correspond to spatial averages in the initially empty and filled sectors of the chain. (c) Breather probability density after a transient of $5 \cdot 10^6$ time units. Data are not collected below the threshold $\eta = 10$. In the three panels the dotted lines refer to homogeneous ICs and $N = 2048$. All data sets have been also averaged over a dozen different realizations of each IC.

tially different macroscopic structures (see the caption of Fig. 5). First we have monitored the evolution of the density of breathers (identified by setting $\eta = 10$). The resulting average results for $N = 4096$ are plotted in Fig. 5a. At variance with the simulations described in Fig. 2, the density appears to converge towards a common finite value, i.e. towards a multi-breather stationary state. Moreover, the dotted line corresponding to a simulation with $N = 2048$ indicates that the asymptotic value of ρ is independent of the system size (and approximately equal to one breather per thousand sites). We have also monitored the temperature. In this model, the standard kinetic definition does not apply, since the Hamiltonian is not decomposable into kinetic and potential energy. Nevertheless, one can use the microcanonical definition, $T^{-1} = \partial S / \partial H$, where S is the thermodynamic entropy and the partial derivative must be computed taking into account the existence of two conserved quantities. This task requires long and careful calculations with a final *non-local* expression [9]. We have preliminarily verified that the definition of [9] works for positive temperatures when applied to the full and to short sub chains. The results in R_n are plotted in Fig. 5b, where one can see that $\beta \equiv 1/T$ converges to a common value for all of the four different classes of ICs (either from above or from below), with negligible finite-size effects (once again the

dotted curve refers to a chain of half length, $N = 2048$). Altogether, one can conclude that on the time scales that are numerically accessible (of order 10^7), the DNLS converges towards a multi-breather state characterized by a finite density of breathers and a well-defined negative temperature.

In practice, what happens is that the breathers are prevented from becoming “too large”. In Fig. 5c, one can indeed see that the pseudo-stationary distribution of breather amplitudes is effectively localized below $a = 22$ and, more importantly, the distribution is basically independent of the system size. Altogether, this means that there is a dynamical process which “screens” the high amplitude region. One can argue that this dynamical effect is due to the low efficiency of the energy-transfer among breathers interacting through the background, a manifestation of their intrinsic dynamical stability. As a consequence, the evolution is “confined” to a region of the phase space that is characterized by a NT. We still expect a convergence towards the equilibrium state predicted in [5] eventually, but the process occurs on such long (unobservable) time scales [17] (further slowed down by coarsening processes) to make it inaccessible. It is nevertheless worth mentioning that if the IC contains one or more sufficiently-high breathers, the amount of energy that they carry is effectively frozen, while the structure of the metastable state depends on the remaining “excess” energy that is still free to diffuse between background and smaller breathers. Altogether, the scenario is quite reminiscent of what happens in spin glasses although a more quantitative analysis is necessary to clarify for example possible aging phenomena.

Generation of NT states. NT states can be generated by moving in parameter space from an initial state in a region where equilibrium is characterized by a homogeneous regime, i.e. positive temperatures. Two particularly simple mechanisms to generate NT states are: localized dissipations with removal of mass (and energy) at the extrema of the chain [11] or a free expansion in lattices of larger size. In the inset of Fig. 1 we show an average trajectory that results from the first method of boundary dissipation in a chain with $N = 200$ sites. The free expansion method from a positive-temperature equilibrium state to a NT state is demonstrated in the upper dot-dashed line in Fig. 5b). From Fig. 1, one can easily realize that a free expansion amounts to decreasing a until the $T = \infty$ line is crossed and the NT region is eventually reached. Thus, in either BECs in optical lattices, or arrays of optical waveguides, this procedure amounts to prepare a standard equilibrium state at $T > 0$ and leave it to spread in sufficiently larger lattice structures. This method is much simpler than the experimental schemes described in [12].

Conclusions. We have explored the dynamical behav-

ior of the DNLS equation in the parameter region corresponding to NT states. Numerical simulations show that for sufficiently uniform initial conditions, the system converges towards a stationary although metastable state characterized by a negative temperature and a finite density of breathers. The asymptotic convergence to the single-breather equilibrium state occurs on much longer (and practically unattainable) time scales. We envisage a quantitative theory that relates the time scales to the breather amplitudes, their stationary density and the system size so as to establish possible connections with, e.g. aging phenomena.

Acknowledgements. RL acknowledges financial support from the Italian MIUR-PRIN project n. 20083C8XFZ and G-LO from the EU Commission FET Open Grant HIDEAS. SI and AP thank T. Carletti for useful discussions on the implementation of symplectic integrators.

-
- [1] P.G. Kevrekidis *The discrete nonlinear Schrödinger equation*, (Springer, Berlin 2009).
 - [2] R. Franzosi, R. Livi, G.-L. Oppo and A. Politi, *Nonlinearity* **24**, R89 (2011).
 - [3] K. Ø. Rasmussen, T. Cretegny, P. G. Kevrekidis and N. Grønbech-Jensen, *Phys. Rev. Lett.* **84**, 3740 (2000).
 - [4] E. M. Purcell and R. V. Pound, *Phys. Rev.* **81**, 279 (1951); N. F. Ramsey, *Phys. Rev.* **103**, 20 (1956).
 - [5] B. Rumpf, *Phys. Rev. E* **69**, 016618 (2004); *Europhys. Lett.* **78**, 26001 (2007); *Phys. Rev. E* **77**, 036606 (2008); *Physica D* **238**, 2067 (2009).
 - [6] G.P. Tsironis and S. Aubry, *Phys. Rev. Lett.* **77**, 5225 (1996).
 - [7] B. Rumpf and A.C. Newell, *Phys. Rev. Lett.* **87**, 54102 (2001).
 - [8] A.J. Bray, *Adv. Phys.* **43**, 357 (1994).
 - [9] R. Franzosi, *J. Stat. Phys.* **143**, 824 (2011).
 - [10] M. Johansson and K.O. Rasmussen, *Phys. Rev. E* **70**, 066610 (2004).
 - [11] R. Livi, R. Franzosi and G.-L. Oppo, *Phys. Rev. Lett.* **97**, 060401 (2006).
 - [12] A. Mosk, *Phys. Rev. Lett.* **95**, 040403 (2005). The scheme was generalised to fermions in A. Rapp, S. Mandt and A. Rosch, *Phys. Rev. Lett.* **105**, 220405 (2010).
 - [13] S. Flach and C. R. Willis, *Phys. Rep.* **295**, 181 (1998); S. Flach and A. V. Gorbach, *Phys. Rep.* **467**, 1 (2008); G. James, *J. of Nonlin. Sciences* **13**, 27 (2003).
 - [14] When we refer to the local amplitude we always refer to the square amplitude.
 - [15] We have selected a sufficiently large threshold to ensure a negligible contribution of the background fluctuations, here expected to follow a Poisson distribution [5].
 - [16] H. Yoshida, *Phys. Lett. A* **150**, 262 (1990).
 - [17] In [10] it was already noticed that a single breather state was evolving so slowly as to converge towards the equilibrium state over 10^{70} time units.